

## Research Article

# Photodegradation of Fleroxacin Injection: Different Products with Different Concentration Levels

Jun Wang,<sup>1,2</sup> Wei Li,<sup>3</sup> Chen-Gui Li,<sup>1,2</sup> and Yu-Zhu Hu<sup>1,2,4</sup>

Received 11 April 2011; accepted 20 June 2011; published online 30 June 2011

**Abstract.** Photodegradation of fleroxacin is investigated in different injections and solutions. After UV irradiation, fleroxacin was degraded to afford two major products in large-volume injection (specification, 200 mg:100 ml), while degraded to afford another major product in small-volume injection (specification, 200 mg:2 ml). The photodegradation products were detected and isolated by reversed-phase HPLC. Based on the spectral data (FT-IR, MS<sup>n</sup>, TOF-MS, <sup>1</sup>H/<sup>13</sup>C, DEPT, and 2D NMR), the structures of these products were: 8-fluoro-9-(4-methyl-piperazin-1-yl)-6-oxo-2,3-dihydro-6H-1-oxa-3a-aza-phenalene-5-carboxylic acid (impurity-I); 6-fluoro-1-(2-fluoro-ethyl)-7-(2-methylamino-ethylamino)-4-oxo-1,4-dihydro-quinoline-3-carboxylic acid (impurity-II); and 6,8-difluoro-1-(2-fluoro-ethyl)-7-(2-methylamino-ethylamino)-4-oxo-1,4-dihydro-quinoline-3-carboxylic acid (impurity-III), respectively. Different photodegradation pathways of fleroxacin were proposed, which led to the different stability characteristics of fleroxacin in the injections. The fluorine atom at C8 is more photolabile in dilute injection, so defluorination and cyclization reactions are prone to take place, whereas photo irradiation only cause ring-opening oxidation reaction of piperazine side chain in concentrated injection.

**KEY WORDS:** elucidation; fleroxacin injection; photodegradation pathway; photodegradation product.

## INTRODUCTION

Fleroxacin, having a chemical name 6, 8-difluoro-1-(2-fluoroethyl)-1, 4-dihydro-7-(4-methyl-1-piperazinyl)-4-oxo-3-quinoline carboxylic acid, is a synthetic fluoroquinolone antibacterial, and the chemical structure of which is shown in Fig. 1. Like other fluoroquinolones, the mechanism of its strong activity against Gram-negative and some Gram-positive strains is based on inhibition of bacterial enzyme DNA gyrase (1). Quinolone antibiotics were relatively stable to high temperature, humidity, and acid. However, many degradation products were found upon exposure to photo irradiation (2). Since drug photodecomposition may result in loss of potency and adverse effects due to the formation of minor degradation products (3), elucidation of impurities is useful for studies on mechanism of photodegradation, structure–phototoxicity relationship (4), and adverse reactions (5) after application of quinolones. Tibirica *et al.* proposed five probable photodegradation products of ciprofloxacin with liquid chromatography mass spectroscopy (LC-MS)/MS (6). Tetsuya *et al.* elucidated

structures of photodegradation products of sitafloxacin and proved dechlorination was the key step in the degradation (7). Yoshida *et al.* (8) elucidated nine photodegradation products of levofloxacin, and they were all analogs altered at the *N*-methylpiperazine moiety. Paola Calza's work showed the transformation of ofloxacin under irradiation with solar light, which was also confined to the piperazine moiety and to the methyl groups (9).

Fleroxacin is instable in injections when exposed to light (10) as many other fluoroquinolones (11). Like lomefloxacin, the fluorine atom at C-8 in the structure of fleroxacin makes it even more photolabile, and more photomutagenic and photocarcinogenic than fluoroquinolones in which C-8 is either unsubstituted or bears a substituent other than fluorine (12). A few liquid chromatographic methods were reported for the determination of fleroxacin in bulk and pharmaceutical dosage forms (13,14). Methods listed in the Chinese Pharmacopoeia (15) address the analysis of fleroxacin in bulk. Additional methods (16–18) describe analysis of biological samples. However, there were few reports concerning fleroxacin that degraded by exposure to light (10). Products of decarboxylation were reported after fleroxacin was degraded by refluxing in hydrochloric acid for 80 h (19), but the isolation and structure elucidation of other photodegradation products were not performed.

Photochemical stability of a drug compound in a formulation should be predicted from the absorption spectrum or stability studies of the drug in the final preparation (20), so the present work studied fleroxacin

<sup>1</sup>Key Laboratory of Drug Quality Control and Pharmacovigilance, Ministry of Education, Nanjing 210009, China.

<sup>2</sup>Department of Analytical Chemistry, China Pharmaceutical University, Nanjing 210009, China.

<sup>3</sup>Department of Antibiotics, Anhui Institute for Food and Drug control, Hefei 230051, China.

<sup>4</sup>To whom correspondence should be addressed. (e-mail: njhuyuzu@126.com)

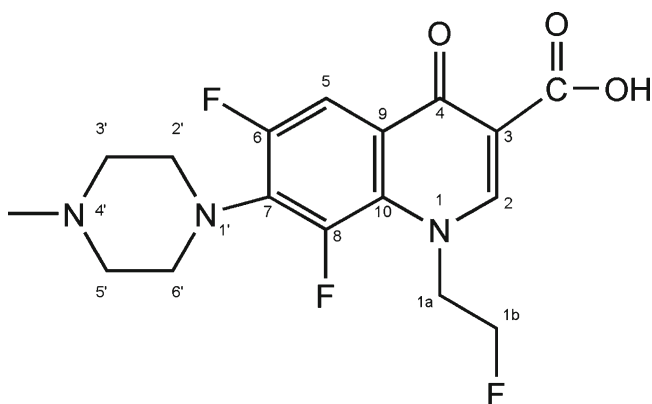


Fig. 1. Structure of fleroxacin

injection exposed to the ultraviolet irradiation, and different degraded products were found in different injections (specification, 200 mg:2 mL and 200 mg:100 mL) due to different concentrations of fleroxacin. The results were demonstrated by an analysis of photo-irradiated fleroxacin solutions with different concentrations prepared. The use of the isocratic reverse high-performance liquid chromatography (HPLC) method detected and isolated the photodegradation products, and then  $^1\text{H}$ ,  $^{13}\text{C}$ , correlation spectroscopy (COSY), heteronuclear single quantum coherence (HSQC), heteronuclear multiple bond correlation (HMBC), nuclear magnetic resonance (NMR), and mass spectrometry techniques elucidated the structure of the three major impurities. Different photodegradation pathways of fleroxacin were proposed. A high concentration of fleroxacin suppressed photo-defluorination reaction at C-8. However, defluorination at C-8 and cyclization reactions were prone to take place in the diluted injection. The results imply that injections at high concentrations are more photo-stable during manufacturing, storage, and application.

## EXPERIMENTAL

### Materials and General Methods

Fleroxacin injection (specification, 100 mL:200 mg of fleroxacin, contains 99.7% of the labeled amount) manufactured by Runbang Pharmaceutical Co., Ltd. (Jiangsu, China), fleroxacin injection (specification, 2 mL:200 mg of fleroxacin, contains 99.9% of the labeled amount) manufactured by Changzheng-cinkate Pharmaceutical Co., Ltd. (Jiangsu, China) were purchased from the market. All chemicals used in this study were of analytical grade or higher. Fleroxacin was supplied from Jinan Limin Pharmaceutical Co., Ltd. (Shandong, China). Solutions of fleroxacin (100 mg/mL) were prepared by weighing 10 g fleroxacin, transferring to a 100-mL volumetric flask, adding 2.5 mL of lactic acid, followed by adding water to make up for volume. Volumes of 3.0, 1.0, 0.5, and 0.2 mL of stock solution (100.0 mg/mL) were transferred to 10-mL volumetric flasks, diluted to the mark with water, yielding concentrations of 30, 10, 5, and 2 mg/mL.

Infrared (IR) spectra were recorded on a Thermo Fisher Fourier transform infrared (FT-IR) IS10 (Waltham, USA) spectrometer. UV spectra were acquired by the photodiode array detector (200–400 nm) as the peaks eluted off the

analytical column. NMR spectra were recorded on a Bruker-Avance 500-MHz spectrometer in DMSO- $\text{D}_6$ +TFA-D. The 2D NMR experiments (COSY, distortionless enhancement by polarization transfer (DEPT), HSQC, and HMBC) were performed using standard Bruker pulse sequences. Analytical HPLC was performed on an Agilent 1200 LC system equipped with a photodiode array detector. The column was an Agilent HC-C18 (250×4.6 mm i.d. packed with 5- $\mu\text{m}$  particle size). The mobile phase consisted of acetonitrile–0.1 mol/L ammonium formate (adjusted to pH 4.2 with formic acid) (15:85, v/v). The flow rate was kept at 0.8 mL/min, and the column eluent was monitored at 286 nm for 50 min. LC/MS data were obtained with a triple quadrupole mass spectrometer equipped with electrospray ionization (ESI) source coupled to an Agilent LC system. The fragmentor voltage was 120. HPLC condition was the same as analytical HPLC condition described above. The scanned  $m/z$  range was 110–1,000 Da. Semipreparative HPLC was performed on an Agilent 1200 LC system equipped with a UV detector (monitoring at 286 nm). The column was Kromasil ODS (5- $\mu\text{m}$  particle size, 250×10 mm i.d., 100 Å; Shanghai Anpel Instrument Co., Ltd.). The weight of the molecule and the most fitting structural formula were performed using a 6520 accurate-Mass-Q-TOF LC/MS system. Data were processed through Agilent MassHunter qualitative analysis.

### Photodegradation Procedure

Photodegradation of fleroxacin solutions was conducted in Pyrex glass cells (50×50×80 mm) of 200 mL capacity. Reaction mixture inside the cell, consisting of 100 mL of Fleroxacin solution, was kept at room temperature and stirred all the time by a magnetic stirrer during the experiment. For photoconversion, the 254-nm line of a low pressure Hg lamp (50 W, Shanghai Hailian Co., Ltd., Shanghai, China) was applied, and the working sample was placed in front of it at a distance of 10 cm. After irradiation, all samples were immediately protected from light with aluminum foil and subjected to HPLC analysis.

### Isolation of Photodegradation Products

After irradiation, the fleroxacin injections were injected onto the semipreparative HPLC column monitoring at UV 286 nm. The effluents at 16.5–18.5 min, 21.1–23.1 min, and 37.4–39.4 min were collected, then refined and desalted for MS, IR,  $^1\text{H}$  NMR, and  $^{13}\text{C}$  NMR spectral analysis.

## RESULTS

### Detection of Impurities

The fleroxacin injections were kept at the ultraviolet irradiation for 1 day and 10 days, then diluted to the same concentration (1 mg/mL) and determined with the analytical LC method. Some impurity peaks could not be separated with the assay method in Chinese Pharmacopoeia, so the mobile phase in this paper was used, and with which the MS detector can be used to monitor the molecular weight and fragments of photodegradation products on line. The analytical method was validated as per ICH guidelines for various parameters such as specificity, precision, linearity,

accuracy, and limit of detection, limit of quantitation, ruggedness, and robustness. After irradiation, a few impurities were found (Fig. 2), and the quantity of the impurities increased as the time of the UV irradiation was prolonged. Fleroxacin injection (specification, 200 mg:100 mL, concentration, 2 mg/mL) exposed to ultraviolet for 1 day mainly produced impurity II, and 87.6% of the labeled amount of fleroxacin remained. After 10 days of ultraviolet irradiation, the peak of fleroxacin disappeared (only 0.5% of the labeled amount of fleroxacin remained) and almost completely converted to

impurity II (Fig. 2). Of the labeled amount, 98.1% and 73.1% of fleroxacin were found in fleroxacin injections (specification, 200 mg:2 mL, concentration, 100 mg/mL) exposed to ultraviolet for 24 h or 10 days, and the major impurity was impurity III. The fleroxacin injections consisted of different supplementary materials, but pH values of all the fleroxacin injections were all about 4.0 according to the solubility of fleroxacin and tolerance of human body. To exclude the interference factors caused by supplementary materials, solutions containing 100 and 2 mg/mL of fleroxacin (adjusted

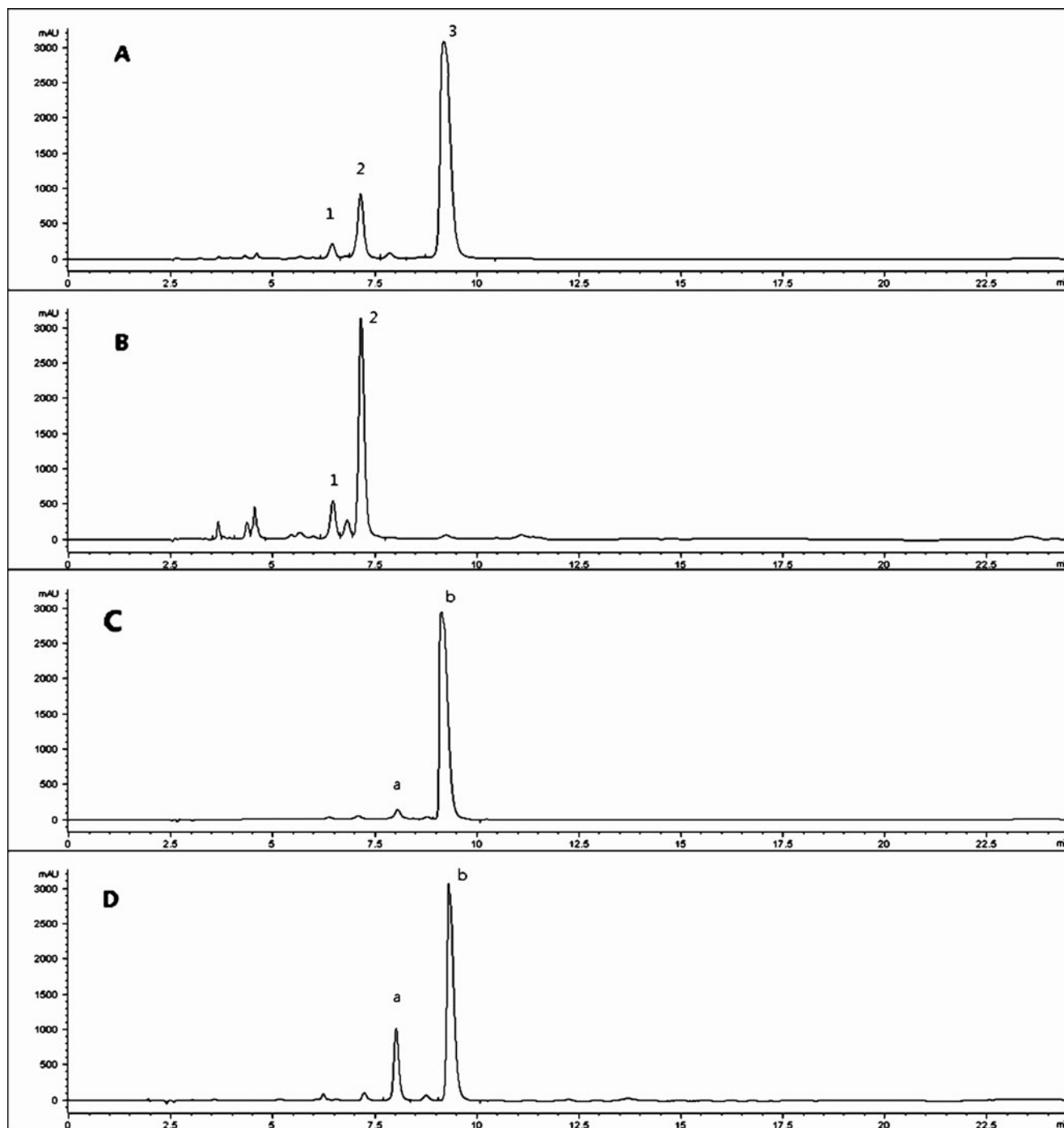


**Fig. 2.** Typical LC chromatogram of fleroxacin injections after UV irradiation. **A** Concentration, 2 mg/mL, irradiated for 1 day; **B** concentration, 2 mg/mL, irradiated for 10 days; **C** concentration, 100 mg/mL, irradiated for 1 day; **D** concentration, 100 mg/mL, irradiated for 10 days; peak 1, impurity-I; peak 2, impurity-II; peak 3, fleroxacin; peak a, impurity-III; peak b, fleroxacin

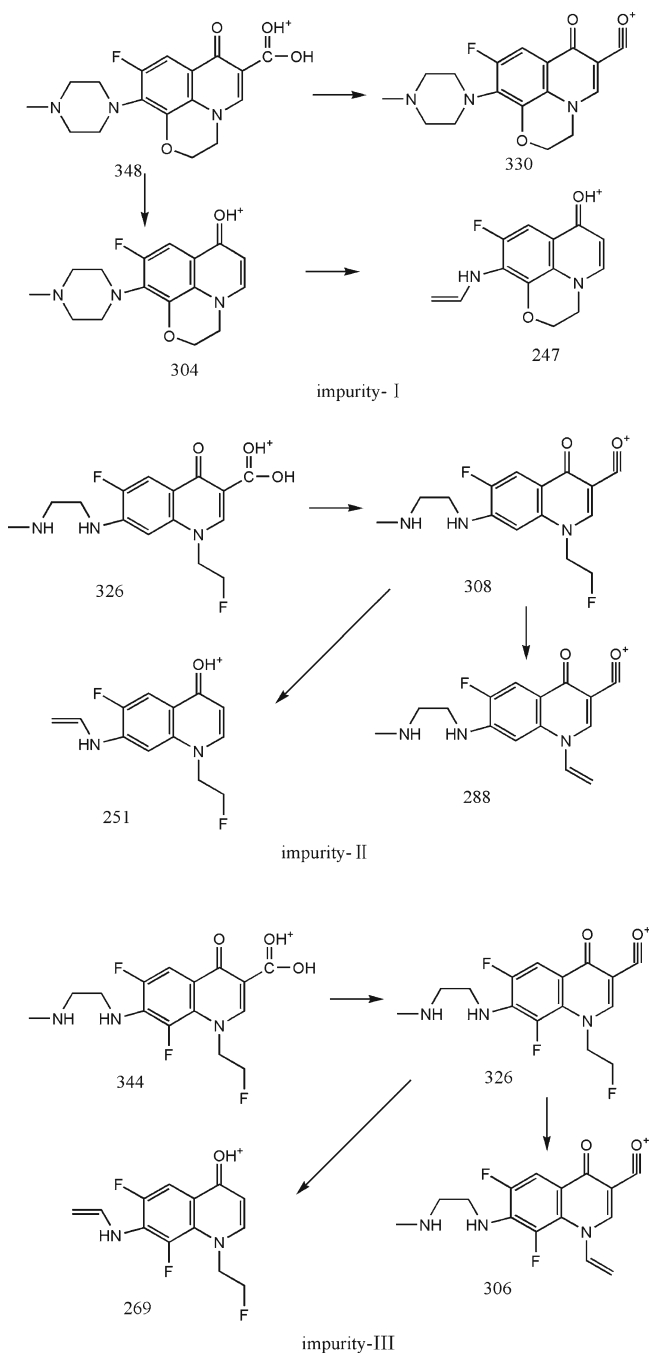


Fig. 3. MS/MS fragmentation pattern of impurity-I, -II, -III

to pH 4.0 with lactic acid) without other additives were prepared, and kept at the ultraviolet irradiation for 1 day and 10 days. HPLC analysis of these solutions showed the same results as the fleroxacin injections. The results imply that solutions at high concentrations are more photo-stable.

### Structural Elucidation of Impurity-I

The isolated impurity-I was found as yellowish green powder and showed similar UV absorbance spectra to parent fleroxacin. The ESI-mass spectroscopy (MS)<sup>n</sup> spectrum of impurity-I showed peaks at  $m/z$  348 amu. The molecular weight of impurity-I was confirmed as 347 Da, 22 Da less than that of fleroxacin. Time of flight mass spectroscopy (TOF-MS) data showed that the molecular weight of impurity-I was 347.1283 Da, the matching molecular formula was  $C_{17}H_{18}FN_3O_4$ . Compared with parent, impurity-I had two "F" less and one "O" more, which was coincident with the loss of atomic mass unit. Based on the spectral information, tentative structure of impurity-I was proposed; the structure and the fragments of the impurity are given in Fig. 3. In the IR spectrum of impurity-I (Table I), a characteristic absorption band appeared at  $3,431\text{ cm}^{-1}$  for  $-\text{OH}$  stretching and  $1,687\text{ cm}^{-1}$  for  $-\text{C}=\text{O}$  stretching of carboxyl.

The  $^1\text{H}$ ,  $^{13}\text{C}$ , and 135 DEPT NMR data of impurity-I and fleroxacin were shown in Tables II and III. The  $^1\text{H}$  NMR spectrum of impurity-I showed that the number of atoms and chemical shift of hydrogen were similar to fleroxacin. At 4.57 and 4.61 ppm, peaks of  $\text{CH}_2$  shifted to the upfield region comparing to fleroxacin. This result was consistent with the structural of impurity-I; the substituent group at C-1b was changed from fluorine atom to oxygen atom, and the electron density of the ethyl decreased.

The  $^{13}\text{C}$  NMR fleroxacin spectrum showed indication of the  $^{19}\text{F}$ - $^{13}\text{C}$  coupling. The five  $^{13}\text{C}$  doublets resonances at 108.47, 128.19, 133.33, 148.65, 154.84 ppm were due to the aromatic carbons of the fluoroquinolone ring coupled to the fluorine atom, but the doublets patterns of aromatic carbons remained three in the  $^{13}\text{C}$  NMR impurity-I spectrum. The remaining  $^{13}\text{C}$  doublets patterns at 58.95, 82.12 ppm observed to fleroxacin, arising from the ethyl carbon atoms coupled by the fluorine atom, disappeared in the impurity-I spectrum. From the data, impurity-I was assigned as 8-fluoro-9-(4-methyl-piperazin-1-yl)-6-oxo-2,3-dihydro-6H-1-oxa-3a-aza-phenalene-5-carboxylic acid.

Table I. FT-IR Spectral Data for Fleroxacin and Photodegradation Products

Sample no.	Compound	IR (KBr)
1	Fleroxacin	3,428( $\gamma_{\text{O-H}}$ ); 3,054( $\gamma_{\text{Ar-H}}$ ); 2,796( $\gamma_{\text{CH}_3\text{-N}}$ ); 1,717( $\gamma_{\text{C=O}}$ ); 1,626; 1,479( $\gamma_{\text{C-O}}$ ); 1,557( $\gamma_{\text{C-C}}$ ); 1,450 ( $\delta_{\text{CH}_3\text{-N}}$ ); 1,281, 1,152( $\gamma_{\text{C-F}}$ ); 1,038 ( $\delta_{\text{O-H}}$ ); 807, 741( $\delta_{\text{Ar-H}}$ )
2	Impurity-I	3,431( $\gamma_{\text{O-H}}$ ); 2,924 ( $\gamma_{\text{Ar-H}}$ ); 2,852( $\gamma_{\text{CH}_3\text{-N}}$ ); 1,681( $\gamma_{\text{C=O}}$ ); 1,575, 1,465( $\gamma_{\text{C-O}}$ ); 1,384( $\delta_{\text{CH}_3\text{-N}}$ ); 1,289, 1,095( $\gamma_{\text{C-F}}$ ); 599( $\delta_{\text{Ar-H}}$ )
3	Impurity-II	3,405( $\gamma_{\text{O-H}}$ ); 2,950( $\gamma_{\text{Ar-H}}$ ); 2,860( $\gamma_{\text{CH}_3\text{-N}}$ ); 1,687( $\gamma_{\text{C=O}}$ ); 1,577, 1,497( $\gamma_{\text{C-O}}$ ); 1,528( $\gamma_{\text{C-C}}$ ); 1,399( $\delta_{\text{CH}_3\text{-N}}$ ); 1,287, 1,168( $\gamma_{\text{C-F}}$ ); 1,056 ( $\delta_{\text{O-H}}$ ); 805, 755( $\delta_{\text{Ar-H}}$ )
4	Impurity-III	3,416( $\gamma_{\text{O-H}}$ ); 2,926( $\gamma_{\text{Ar-H}}$ ); 2,865( $\gamma_{\text{CH}_3\text{-N}}$ ); 1,679( $\gamma_{\text{C=O}}$ ); 1,636, 1,485( $\gamma_{\text{C-O}}$ ); 1,548( $\gamma_{\text{C-C}}$ ); 1,423( $\delta_{\text{CH}_3\text{-N}}$ ); 1,286, 1,199( $\gamma_{\text{C-F}}$ ); 1,039 ( $\delta_{\text{O-H}}$ ); 806, 721( $\delta_{\text{Ar-H}}$ )

**Table II.**  $^1\text{H}$  Data for Fleroxacin and Photodegradation Products

Position	Fleroxacin			Impurity-I			Impurity-II			Impurity-III		
	$^1\text{H}$	$\delta$ (ppm)	M*	$^1\text{H}$	$\delta$ (ppm)	M*	$^1\text{H}$	$\delta$ (ppm)	M*	$^1\text{H}$	$\delta$ (ppm)	M*
2	1	8.80	s	1	8.83	s	1	8.79	s	1	8.80	s
5	1	7.86–7.89	d	1	7.62–7.64	d	1	7.90–7.92	d	1	7.81–7.84	d
8	–	–	–	–	–	–	1	6.91–6.93	d	–	–	–
2'	2	3.63–3.71	m	2	3.57–3.60	m	2	3.74–3.76	t	2	3.70–3.73	t
3'	2	3.27–3.61	brm	2	3.24–3.54	brm	2	3.29–3.30	t	2	3.14–3.17	t
5'	2	3.27–3.61	brm	2	3.24–3.54	brm	–	–	–	–	–	–
6'	2	3.63–3.71	m	2	3.57–3.60	m	–	–	–	–	–	–
1a	2	4.87–4.92	m	2	4.57–4.58	m	2	4.82–4.84	m	2	4.82–4.86	m
1b	2	4.93–4.97	m	2	4.61–4.63	m	2	4.87–4.93	m	2	4.89–4.94	m
4'N-CH <sub>3</sub>	3	2.98	s	3	2.94	s	3	2.71	s	3	2.72	s

Assignments made on the basis of DEPT, COSY, HSQC, and HMBC experiments  
*s* singlet, *d* doublet, *t* triplet, *m* multiplet, *brm* broad multiplet, *M\** multiplicities

### Structural Elucidation of Impurity-II

The isolated impurity-II was found as yellowish powder. In comparison with parent, the maximal UV absorbance wavelength of impurity-II shifted to the blue region. The ESI-MS<sup>n</sup> spectrum of impurity-II showed peaks at *m/z* 326 amu. The molecular weight of impurity-II was confirmed as 325 Da, 44 Da less than that of fleroxacin. TOF-MS data showed that the molecular weight of impurity-II was 325.1240 Da, the matching molecular formula was C<sub>15</sub>H<sub>17</sub>F<sub>2</sub>N<sub>3</sub>O<sub>3</sub>. Compared with the parent, impurity-II had two “C,” one “H,” and one “F” less, which was coincident with the loss of atomic mass unit. Based on the spectral information, tentative structure of impurity-II was proposed; the structure and the fragments of the impurity are given in Fig. 3. In the FT-IR spectrum of impurity-II (Table I), a characteristic absorption band appeared at 3,405 cm<sup>-1</sup> for –O–H stretching and 1,687 cm<sup>-1</sup> for –C=O stretching of carboxyl.

The <sup>13</sup>C NMR data (Table III) showed that the methylene signal at  $\delta$  54.59 ppm and  $\delta$  48.58 ppm, observed in fleroxacin (corresponded to C-5' and C-6'), was absent in

the impurity-II spectrum. The DEPT spectra showed there were one CH<sub>3</sub>, four CH<sub>2</sub>, and three CH in impurity-II. In fleroxacin, the F atom at C-8 made the electron density of C-7 and C-10 increase, and the chemical shift of C-7 and C-10 decreased correspondingly ( $\delta$  133.33 and  $\delta$  128.19). In impurity-II, the F atom at C-8 was absent, so the  $\delta$  of C-7 and C-10 shifted to the lower field ( $\delta$  143.98 and  $\delta$  140.35). The broken band of piperazin made the number of substituent alkyl on the N-4' and N-2' decrease, which induced the chemical shift of the CH<sub>3</sub> attached to N-4' decreased correspondingly ( $\delta$  43.68→ $\delta$  33.94). And the chemical shift of C-2' ( $\delta$  48.58→ $\delta$  39.93) and C-3' ( $\delta$  54.59→ $\delta$  48.39) decreased for the same reason. From the data, impurity-II was assigned as 6-fluoro-1-(2-fluoro-ethyl)-7-(2-methylamino-ethylamino)-4-oxo-1,4-dihydro-quinoline -3-carboxylic acid.

### Structural Elucidation of Impurity-III

The isolated impurity-III was found as yellowish powder. In comparison with parent, the maximal UV absorbance wavelength of impurity-III shifted to the blue region. The ESI-MS<sup>n</sup>

**Table III.**  $^{13}\text{C}$  Data for Fleroxacin and Photodegradation Products

Position	Fleroxacin ( $\delta$ (ppm))	Impurity-I ( $\delta$ (ppm))	Impurity-II ( $\delta$ (ppm))	Impurity-III ( $\delta$ (ppm))
2	153.28	148.13	150.06	152.11
3	108.31	107.76	107.91	106.77
4	177.00	177.76	176.99	176.04
5	108.47–108.66 (d)	104.15–104.34 (d)	110.60–110.76 (d)	107.03–107.25 (d)
6	154.84–154.89 (d)	155.69–155.81 (d)	150.73–150.84 (d)	156.23–156.26
7	133.33–133.44 (d)	131.20–131.31 (d)	143.98–144.09 (d)	133.31–133.40 (d)
8	148.65–148.70 (d)	142.50	97.44	148.81–148.84
9	123.14	122.20	116.53	118.22
10	128.19–128.24 (d)	126.68	140.35	127.57–127.63 (d)
3-COOH	166.62	167.41	168.53	166.09
2'	48.58	48.22	39.93	40.98
3'	54.59	54.70	48.39	48.92
5'	54.59	54.70	–	–
6'	48.58	48.22	–	–
1a	58.95–59.07 (d)	50.38	55.17–55.32 (d)	58.13–58.39 (d)
1b	82.12–83.50 (d)	65.24	81.83–83.17 (d)	81.42–82.81 (d)
4'N-CH <sub>3</sub>	43.68	43.61	33.94	33.14

Assignments made on the basis of DEPT, COSY, HSQC, and HMBC experiments  
*d* doublet

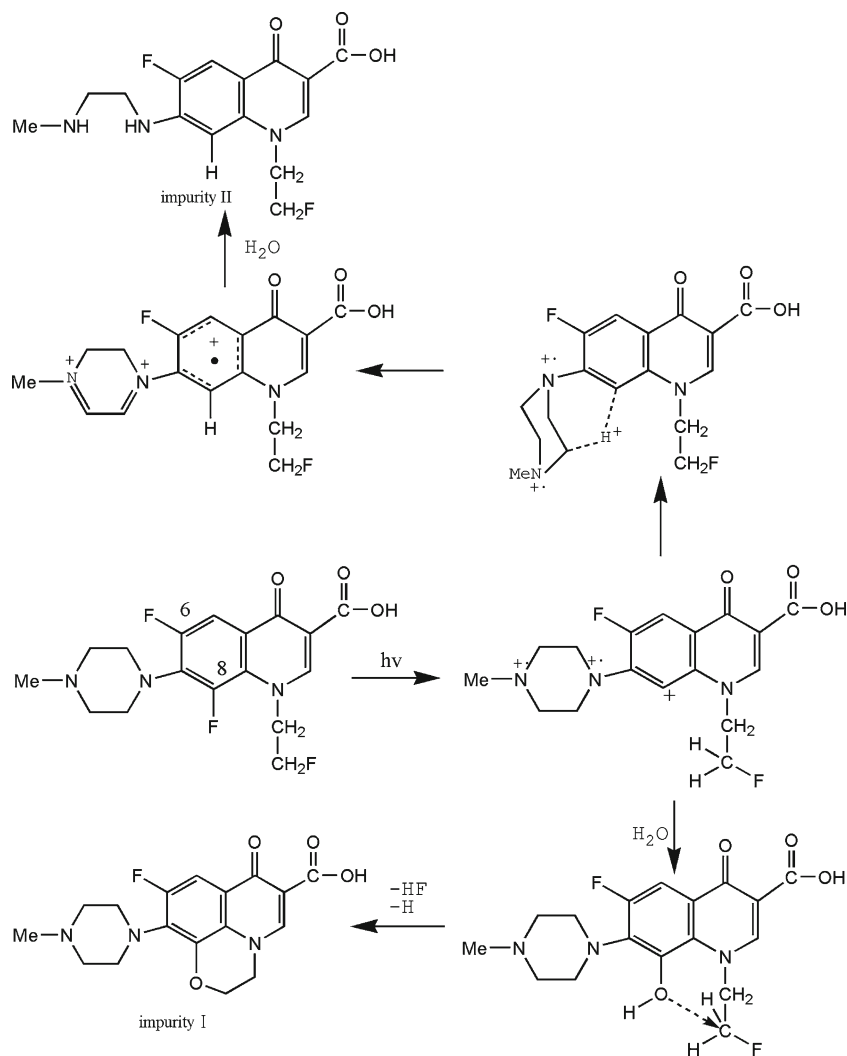


Fig. 4. Photodegradation pathway of fleroxacin in dilute solution

spectrum of impurity-III showed peaks at  $m/z$  344 amu. The molecular weight of impurity-III was confirmed as 343 Da, 26 Da less than that of fleroxacin. TOF-MS data showed that the molecular weight of impurity-III was 343.1121 Da, the matching molecular formula was  $C_{15}H_{16}F_3N_3O_3$ . Compared with parent, impurity-III had two "C" and two "H" less, which was

coincident with the loss of atomic mass unit. Based on the spectral information, a tentative structure of impurity-III was proposed, the structure and the fragments of the impurity are given in Fig. 3. In the FT-IR spectrum of impurity-III (Table I), a characteristic absorption band appeared at  $3,416\text{ cm}^{-1}$  for  $-O-H$  stretching and  $1,679\text{ cm}^{-1}$  for  $-C=O$  stretching of carboxyl.

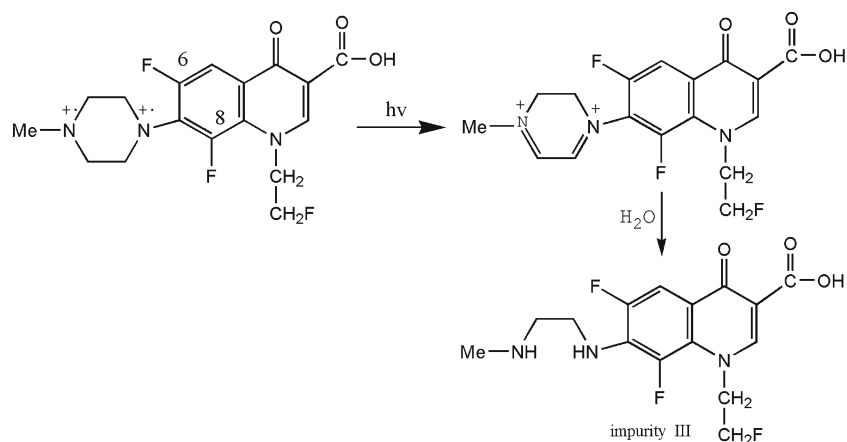


Fig. 5. Photodegradation pathway of fleroxacin in concentrated solution

The  $^{13}\text{C}$  NMR data (Table III) showed that the methylene signal at  $\delta$  54.59 ppm and  $\delta$  48.58 ppm, observed in feroxacin, was absent in the impurity-III spectrum. The DEPT spectra showed that there were one  $\text{CH}_3$ , four  $\text{CH}_2$ , and two CH in impurity-III. The broken band of piperazin made the number of substituent alkyl on the N-4' and N-2' decrease, which induced the chemical shift of the  $\text{CH}_3$  attached to N-4' decreased correspondingly ( $\delta$  43.68  $\rightarrow$   $\delta$  33.14). From the data, impurity-III was assigned as 6,8-difluoro-1-(2-fluoro-ethyl)-7-(2-methylamino-ethylamino)-4-oxo-1,4-dihydro-quinoline-3-carboxylic acid.

## DISCUSSION

Solutions containing 100, 30, 10, 5, and 2 mg/mL of feroxacin were kept at ultraviolet irradiation for 24 h. Results of the HPLC analysis showed that the higher the concentration of the solution, the lesser the amount of impurities was produced under the same irradiation condition. When the concentration of feroxacin was above 10 mg/mL, the major photoproduct was impurity-III, whereas the major photoproduct was impurity-II when the concentration was 5 or 2 mg/mL.

It is likely that photodegradation processes in small-volume injection and large-volume injection are different. In dilute solution, the fluorine atom at C-8 is more photolabile and prone to lose. Cleavage of C-F bond took place first, and then ring-opening reaction of piperazine side chain and cyclization reactions followed. That is the reason for the formation of impurity-I and impurity-II. However, in the concentrated solution of feroxacin containing large amounts of solute molecules, outer molecules block transmission of light and protect inner molecules from light effects, and at the same time, gathered feroxacin molecules caused steric hindrance, so the fluorine atom at C-8 is hard to lose, then more light energy is consumed for the ring-opening oxidation reaction of piperazine side chain at C-7, which is manifested in higher stability of concentrated injections. The two plausible degradation pathways are shown in Figs. 4 and 5.

## CONCLUSION

In this work, photodegradation of feroxacin in small-volume injection and large-volume injection was performed. Three major photodegradation products of feroxacin were isolated and characterized by HPLC-MS and NMR techniques. Significant differences in photodegradation process and photostability between concentrated injection and dilute injection have been demonstrated, which were not described in literature till now. Considering the obtained results, it is important for further studies on adverse effects of the pharmaceutical, impurity profile control, and different photodegradation pathways of feroxacin.

## ACKNOWLEDGMENTS

The author wishes to thank Mr. Wen-Bin Shen (Center of Testing and Analysis, China Pharmaceutical University) for the NMR spectra, Mrs. Jun Chen (Key laboratory of Modern Chinese Medicines China Pharmaceutical University Ministry of Education) for the TOF-MS measurement.

## REFERENCES

- Cullmann W, Geddes AM, Weidekamm E, Urwyler H, Brausteiner A. Fleroxacin: a review of its chemistry, microbiology, toxicology, pharmacokinetics, clinical efficacy and safety. *Int J Antimicrob Agents*. 1993;2:203-30.
- Albini A, Monti S. Photophysics and photochemistry of fluoroquinolones. *Chem Soc Rev*. 2003;32:238-50.
- Castell JV, Gomez MJ, Miranda MA, Morera IM. Photolytic degradation of ibuprofen. Toxicity of the isolated photoproducts on fibroblasts and erythrocytes. *Photochem and Photobiol*. 1987;46:991-6.
- Norihiro H, Yoshihiro N, Akira Y. New findings on the structure-phototoxicity relationship and photostability of fluoroquinolones with various substituents at position 1. *Antimicrob Agents Chemother*. 2004;48:799-803.
- Laurent M, Jean PB, Christophe J, Phillipe P, Lydia R, Alain S, *et al*. Molecular responses to photogenotoxic stress induced by the antibiotic lomefloxacin in human skin cells: from DNA damage to apoptosis. *J Invest Dermatol*. 2003;121:596-606. doi:10.1046/j.1523-1747.2003.12422.x.
- Tibirica GV, Danielle MH, Armin K, Ayrton FM, Klaus K. Photo-degradation of the antimicrobial ciprofloxacin at high pH: Identification and biodegradability assessment of the primary by-products. *Chemosphere*. 2009;76:487-93. doi:10.1016/j.chemosphere.2009.03.022.
- Tetsuya A, Yukinori K, Ikumi O, Hiroaki K. Photochemical behavior of sitafloxacin, fluoroquinolone antibiotic, in an aqueous solution. *Chem Pharm Bull (Tokyo)*. 2002;50:229-34.
- Yoshida Y, Sato E, Moroi R. Photodegradation products of levofloxacin in aqueous solution. *Arzneimittelforschung*. 1993;43:601-6.
- Paola C, Claudio M, Francesco C, Valeria G, Claudio B. Characterization of intermediate compounds formed upon photoinduced degradation of quinolones by high-performance liquid chromatography/high-resolution multiple-stage mass spectrometry. *Rapid Commun Mass Spectrom*. 2008;22:1533-52. doi:10.1002/rcm.3537.
- Djurđević P, Laban A, Jelikić-Stankov M. Validation of an HPLC method for the determination of feroxacin and its photodegradation products in pharmaceutical forms. *Ann Chim*. 2004;94:71-83.
- Tiefenbacher EM, Haen E, Przybilla B, Kurz H. Photodegradation of some quinolones used as antimicrobial therapeutics. *J Pharm Sci*. 1994;83:463-7.
- Martinez LJ, Li G, Chignell CF. Photogeneration of fluoride by the fluoroquinolone antimicrobials agents lomefloxacin and feroxacin. *Photochem Photobiol*. 1997;65:599-602.
- Hérida RNS, Andréia M, Sanjay G. LC-DAD determination of feroxacin in bulk and pharmaceutical dosage forms. *Chromatographia*. 2009;69:237-40. doi:10.1365/s10337-009-1053-8.
- Stuck AE, Kim DK, Frey FJ. Fleroxacin clinical pharmacokinetics. *Clin Pharmacokinet*. 1992;22:116-31.
- Chinese Pharmacopoeia Commission. *Chinese pharmacopoeia*, vol. II. Beijing: Chemical Industry Press; 2005.
- Hobara N, Kameya H, Hokama N, Ohshiro S, Sakanashi M. Rapid and simple determination of feroxacin in rat plasma using a solid-phase extraction column. *J Chromatogr B: Biomed Sci Appl*. 1997;703:279-83.
- Champan JS, Geogppapadakou NH. Fluorometric assay for feroxacin uptake by bacterial cells. *Antimicrob Agents Chemother*. 1989;33:27-9.
- Carlucci G. Analysis of fluoroquinolones in biological fluids by high-performance liquid chromatography. *J Chromatogr A*. 1998;812:343-67.
- Gu H, Sun L, Wu M, Tao Z, Zhao H. the structure identification of degradation product of quinolone drugs. *Chin J Pharm Anal*. 1997;17:89-92.
- Hanne HT. Formulation and stability testing of photolabile drugs. *Int J Pharm*. 2001;225:1-14.